INFLUENCE OF CASTING RATE ON PRECIPITATION OF PARTICLES BASED ON MICRO-ALLOYING ELEMENTS IN SLAB SURFACE ZONE

M. Longauerová, P. Bekeč, M. Fedorová, S. Longauer
Technical University of Košice, Faculty of Metallurgy, Department of Material Science, Slovakia

Received 06.04.2011
Accepted 13.09.2011

Corresponding author: M. Longauerová, Technical University of Košice, Faculty of Metallurgy, Department of Material Science, Park Komenského 11, 042 01 Košice, Slovak Republic, E-mail: margita.longauerova@tuke.sk

Abstract
The aim of this paper was to evaluate the dependence of precipitation on casting rate in the surface zone of a TiNb microalloyed steel slab, and to compare the results with those in a TiNb IF steel slab. In the microalloyed steel TEM revealed fine and larger globular particles and larger angular particles of TiN and TiC. For higher casting rates TEM revealed more fine particles of similar shape, but NbC was combined with TiN and TiC. Precipitates in the slab surface zone of the TiNb IF steel were both globular and oval. They were based on Al and Ti in combination with MnS and stick shape particles based on Al. Comparison of precipitates in the surface zone of slabs cast at the same pulling rate 0.8m/min for both TiNb micro-alloyed steel and TiNb IF steel grades, showed fewer particles in the IF steel. This is assumed to be due to the very low carbon content in the IF steel compared to the microalloyed one.

Keywords: Precipitation, slab, casting rate, TiNb microalloy steel, TiNb IF steel

1 Introduction

Different types of precipitates can be formed by crystallization during continuous casting. There are large differences in the way they influence the quality of continuous casting products. The production of precipitates during continuous casting is influenced strongly by the cooling and solidification in the crystallizer, and also by secondary cooling and cooling after the exit from the casting machine [1]. In addition to this, the precipitation type, whether based on microalloying elements or impurities, its extent, amount and distribution in continuously-cast semis, depends on the steel grade, i.e. the chemical composition and type of microalloying elements and impurities and their segregation [2]. Reviews [3, 4] have shown that transverse cracking formation is influenced by the size and distribution of the microalloy precipitates, and also by precipitated aluminium nitride (AlN) at the grain boundaries. As reported by Ludlow [1], the morphology of the produced precipitates can significantly influence the surface cracking of the casting. Even small volumes of cuboid or rod-shaped precipitates can evoke the formation of surface cracking. Globular precipitates can influence surface cracking only in cases when they are very large in size, and at high volumes in the steel. Precipitates arranged in strings on the original grain boundaries (i.e. those within the final grain matrix), regardless of their shape, can cause surface cracking in probably the same way as precipitates arranged on the final grain boundaries. The effect of elliptic precipitates is distinctly worse, even when significantly smaller in size and amount, than the effect of globular types. As already noted, the cooling in the crystallizer and all the subsequent cooling has a strong influence on the morphology of precipitated particles.

Niobium, titanium and additional microalloying elements in steels are known to influence the recrystallization [2, 5-10], phase transformation [11], grain size [9,12] and welding of high-quality steels [13, 14], such as high-strength low-alloy steels (HSLA) or interstitial-free (IF) steels. Depending on the temperature, these elements can create a whole range of compounds in microalloyed steels, such as TiN, TiC, Ti(CN), NbC, NbN or Nb(CN). In addition to the above particles IF steels can also contain TiS, $Ti_4C_2S_2$, MnS and AlN, but also precipitates with phosphorus, such as $M_xC_yS_zP$, FeTiP [15]. The VNbTi steel exhibited significantly greater precipitation of carbonitrides such as triplex and duplex types based on Ti, Nb and V compared with the V steel, where V(CN) were found [16]. They were characterized in this study by cuboid (45-70 nm), spherical/irregular (20-45 nm) and fine/needlelike (10-20 nm) morphologies. Apart from large cuboidal TiN precipitates in the NbVTi steel, another study [17] also confirmed type I dendritic precipitates (up to 10μm), or type II dendritic precipitates. Large cuboidal precipitates (>0.5μm) formed in the liquid have no grain size refining effect either during reheating before controlled rolling or in HAZ, and these remove titanium and niobium from austenite, thus reducing furher precipitation. Similarly the type I dendritic precipitates are stable at least up to 1150^{o}C and have no grain size refining effect. Type I precipitates form in the interdendritic liquid and these are TiN-rich (TiNb)(CN) in NbVTi steel and NbC-rich (TiNb(CN) in NbTi steel. Type II precipitates nucleate on (TiNb)N at the final stage of solidification of the interdendritic liquid, or on δ–phase boundaries and grow in the solid. The particles are TiN-rich (TiNb)(CN) in NbVTi steel and NbC-rich (TiNb(CN) in NbTi steel. Only type II dendritic precipitates are unstable at 1050^{o}C (for NbV steel) or 1100^{o}C (for NbVTi steel). The precipitates in the case of NbVTi steel are broken into many small pieces at 1100^{o}C and in the HAZ simulation condition and thus they may be useful in grain size refinement [17]. Jun et al. [18] also observed three types, i.e. dendritic, semi-dendritic and rod-like Nb-rich (NbTi)(CN)complex carbonitrides in continuously-cast NbTi-bearing steel. Complex carbonitrides precipitated in the base metal and heat-affected zone (HAZ) in NbTi hot-rolled microalloyed steel plates have also been identified as being Ti-rich (NbTi)(CN) [19]. They had cuboidal shape, and their average particle size in the base metal upon decrease of the reheating temperature from 1200 to 1150^{o}C decreased from 40 to 20nm. The morphology of carbonitrides in the HAZ is transformed from cuboidal to rectangle shape with length of over 500 nm.

Since the influence of casting rate on precipitation in the slab surface zone has not been studied thoroughly, the aim of this contribution was to analyze this influence in TiNb microalloyed steel and compare the results of precipitation with those in TiNb IF steel.

2 Experimental material and methods

Two steel grades were used for the study and comparison of precipitation: TiNb microalloyed steel and TiNb IF steel. Both were microalloyed with Ti and Nb and their chemical compositions are shown in **Tables 1** and **2**.

Table 1 Chemical composition of the microalloyed steel heat [wt. %]

C	**Mn**	**Si**	**P**	**S**	**Al**	**Mo**	**Ti**	**V**	**Nb**
0.076	0.468	0.013	0.01	0.0061	0.024	0.002	0.017	0.001	0.018
B	**Ca**	**Cu**	**Ni**	**As**	**Sn**	**Sb**	**Cr**	**Zn**	**N**
0.0002	0.0002	0.021	0.012	0.005	0.002	0.002	0.012	0.001	0.0042

Table 2 Chemical composition of IF steel [wt. %]

C	Mn	Si	P	S	Al	Ti	V	Nb	Cu	B	N
0.005	0.275	0.009	0.008	0.015	0.05	0.051	0.001	0.048	0.032	0.0002	0,0089

For the TiNb microalloyed steel, samples were produced from slab surface cut outs, from the small radius “r” side of the slab. In the secondary cooling zone the cooling rate of the slab was controlled by the program for microalloyed steel. Two casting rates were tested, specifically accomplished by two pulling rates. The cut outs were labelled in the following way:

- Cut out K-1 (side cut out) and L-2 (central cut out): pulling rate 0.5m/min.
- Cut out M-3 (side cut out) and N-4 (central): pulling rate 0.8m/min.

In this study central samples were used from L-2 and N-4, as shown in **Fig.1**. The continuously-cast slab specifications were as follows:

- Slab dimensions 7360 x 1540 x 220 mm
- Liquidus temperature 1527°C
- Cooling rate control curve for microalloyed steel, producing a moderate cooling rate in the secondary cooling zone

IF steel samples produced from 3 cut-outs across the slab width were used. The pulling rate was 0.8m/min. Steel produced in an oxygen-blowing converter was used. The chemical composition was designed for subsequent vacuum treatment, combined with inert argon blowing. The steel prepared this way was then continuously cast in a curved-type casting machine. The steel samples produced from 3 cut-outs across the slab width were cut from the small radius “r” side as shown in **Fig. 2**. The slab specifications were as follows:

- Slab dimensions: 220 x 1195 mm
- Liquidus temperature 1532 ºC
- Casting temperature 1561ºC
- Cooling rate control in the secondary cooling zone - moderate

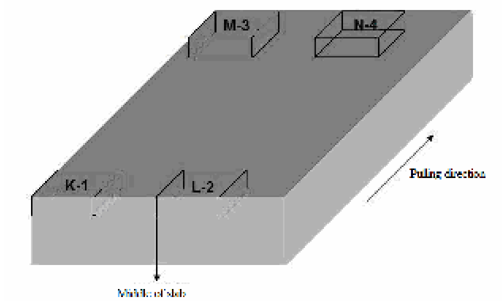

Fig.1 Cut outs from TiNb microalloyed steel slab

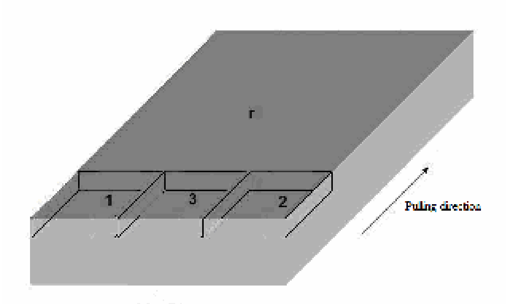

Fig.2 Cut-out from IF steel slab

Transmission electron microscopy (TEM) with a JEOL JEM 2000 FX microscope was used to study the precipitates, applying the carbon replica method. The particles were identified by EDX analysis using a LINK 860 analyzer, by electron diffraction in the extracted replicas and EELS method.

For TiNb microalloyed steel carbon replicas were analysed extracted from samples L3 and L4, which were selected from the central cut-out L-2 of the slab. The pulling rate was 0.5m/min. Sample N9 was analysed, also selected from the central cut-out N-4 of the slab pulled with higher pulling rate 0.8m/min. The carbon replicas were produced in surfaces cut in a direction parallel to the surface and 2 to 2.5 mm deep under the slab surface.

For IF steel carbon replicas were extracted from all 3 cut-outs. The samples about 3 mm deep from the slab surface were dusted with carbon, and replicas were extracted.

3 Results and discussion

TiNb micro-alloyed steel

Carbon replica observation of samples L3 and L4 produced from the central cut-out L2 of the slab pulled at the lower rate 0.5m/min revealed a number of smaller and larger globular particles and large angular ones. More of the latter were seen in sample L4. The observed particles are documented in **Figs. 3** and **4** for sample L3 and in **Figs. 5** and **6** for sample L4. The types of particles with size ranges are listed in **Tab. 3**. In sample L3 the sizes of fine globular particles ranged from 3.8 to 11.5 nm, and the sizes of large globular particles ranged from 15.4 to 76.9 nm. The 2 angular particles were 76.9 – 107.7 nm in size. EDX analysis of sample L3 showed particles based on Ti and Nb (**Fig.7**). Diffraction plot analysis showed a TiN particle. Globular and angular particles were observed in sample L4 (Figs. 5 and 6). The sizes of fine globular and oval particles ranged from 4.8 to 9.5 nm. The sizes of the larger globular particles were from 12.5 to 18.7 nm and the angular particle size was from 14.3 to 75 nm. The number of angular particles in sample L4 was considerably higher compared to L3. This gives evidence of precipitation heterogeneity in the slab surface zone, though these two samples were close to one another. EDX analysis of the angular particle revealed a composition based on S, Ti and Nb (Fig.8). EDX analysis of one other particle from sample L4 also confirmed Ti and Nb. Diffraction plot results showed particles TiN and TiC.

Table 3 Precipitated particle size evaluation

Shot Number	Sample	Fine globular particles [nm]	Large globular particles [nm]	Large angular particles [nm]
839	L3	7.7	15.4 – 76.9	76.9 – 107.7
837	L3	3.8 – 11.5	15.4 – 38.5	
836	L4		12.5 – 18.7	37.5 – 75
832	L4	4.8 – 9.5		14.3 – 61.9
840	N9	9.5	14.3 – 28.6	47.6 – 71.4
841	N9	6.3 – 9.4	12.5 – 28.1	

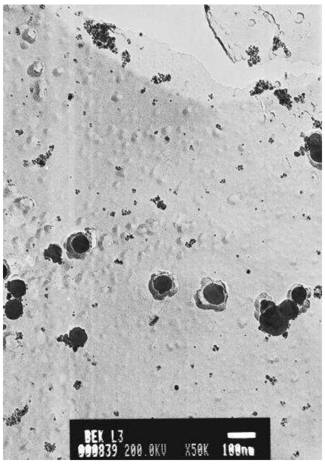

Fig.3 Fine and large globular particles, sample L3, Magnification 50 000x

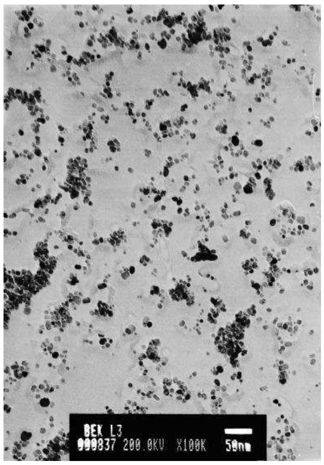

Fig.4 Globular particles, sample L3, Magnification 100 000x

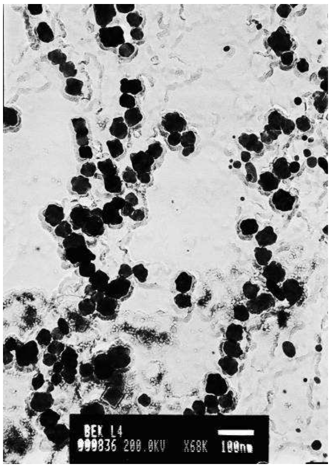

Fig.5 Mainly large globular and angled particles, sample L4, Magnif.68 000x

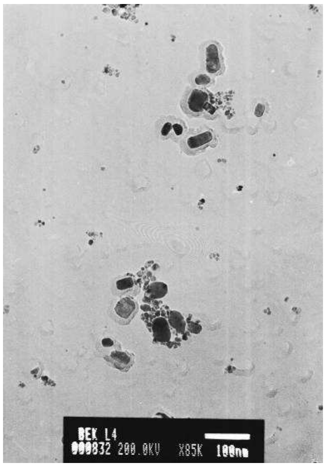

Fig.6 Fine globular and large angular particles, sample L4, Magnif.85 000x

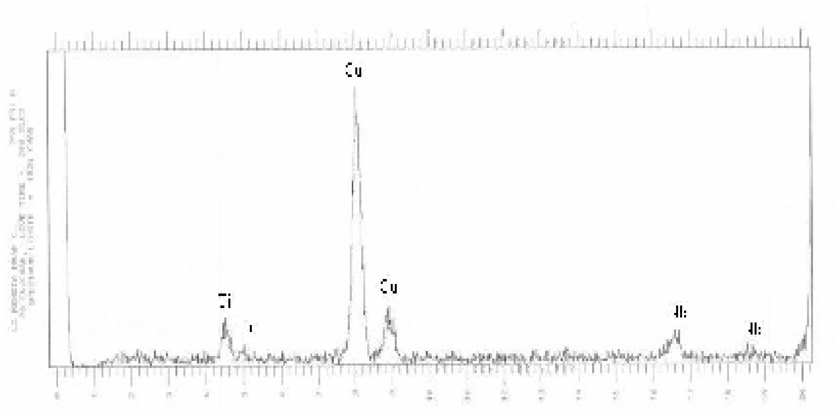

Fig.7 Smaller angular particle EDX analysis, sample L3

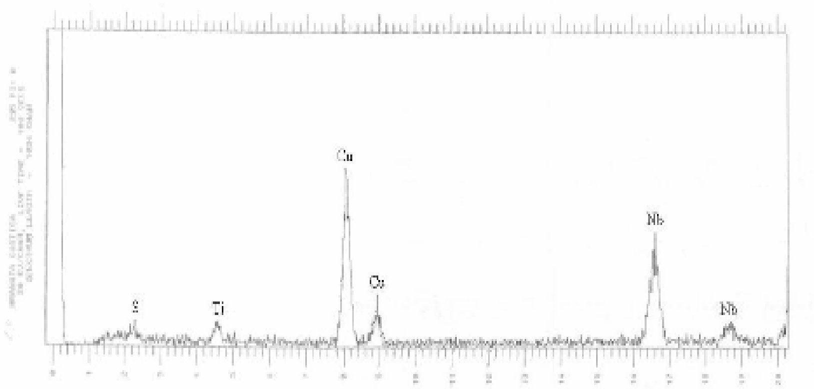

Fig.8 Angular particle EDX analysis, sample L4

Sample N9 was cut out from the slab cast at the higher casting rate, actually pulled at a rate of 0.8m/min. Carbon replicas extracted from sample N9 revealed small globular and oval particles, with sizes ranging from 6.3 to 9.5 nm (**Fig.9**). Some solitary large particles were there too, globular (12.5 – 28.6 nm) or angular (47.6 – 71.4 nm) (Fig.10). The results of the EDX analysis of the fine precipitated particles showed Ti and Nb. According to the diffraction results, the particles were TiC and NbC combined with TiN.

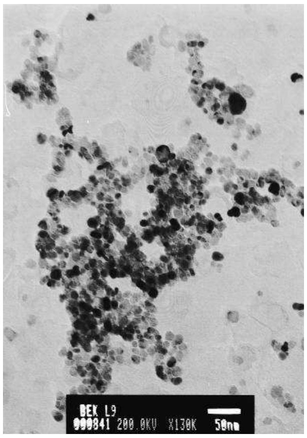

Fig.9 Small globular or oval particles, sample N9, Magnif.130 000x

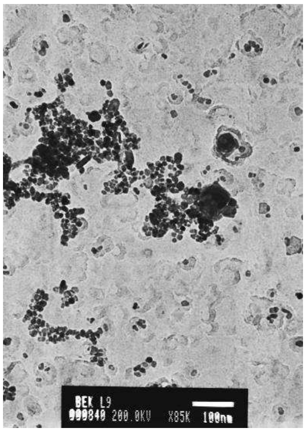

Fig.10 Small globular and single angular particle, sample N9, Magnif.85 000x

TiNb IF steel

Carbon replica observation of a sample produced from the left side cut-out 1 of the slab showed globular and oval particles in a ferrite matrix (**Fig.11**). Their sizes ranged from 28 to 71nm. The pulling rate of the slab was 0.8 m/min. The EDX analysis results showed some complex particles with Al and Ti (**Fig.12**). In sample 3 from the central cut-out the size of the particles found ranged from 14 to 85.7 nm (**Fig.13**). The EELS analysis indicated nitride particles of Al and Ti. **Fig.14** is the documentation of stick-like particles found deeper under the slab surface (20 mm). They were Al based and their sizes ranged from 71 nm to 114 nm.

Fig.11 TEM, globular particles, cut-out 1, Magnif.74 200 x

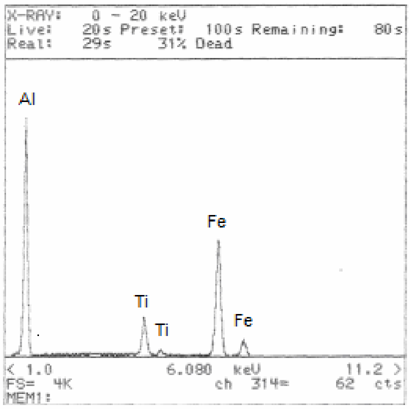

Fig.12 EDX spectrum

Fig.13 TEM, dispersed globular particles, cut-out 3, Magnif.78 600 x

Fig.14 Stick shape particles, cut-out 3, Magnif.75 700 x

The obtained EDX spectrum confirmed in the sample from the right side cut out 2, particles based on Ti and Al. There was heterogeneity in the size of the particles and in places there were precipitates arranged in strings. There were very fine particles ranging from 4.1 nm to 41.6 nm in size, and larger particles from 57.1 to 100 nm. EDX analysis of the polished surface confirmed very fine cementite particles as well, and also large complex TiCN particles up to 160 nm in size, sometimes in combination with MnS deeper under the slab surface.

Comparison of the precipitates in the tested steels showed differences in the distribution and size of particles. In micro-alloyed TiNb steel there were large numbers of particles, but in the TiNb IF steel the number of particles was smaller. This may have contributed to the very low carbon content in the IF steel compared to the micro-alloyed. This remains to be proven, however, requiring a large number of samples and statistics on them.

4 Conclusion

The precipitation evaluation in the surface zone of slabs made from TiNb micro-alloyed steel produced at two different casting rates and from TiNb IF steel led to the following conclusions:

1. Samples taken 2.5 mm deep in the TiNb micro-alloyed steel slab with low pulling rate 0.5m/min revealed fine globular particles up to 11.5 nm in size and larger globular particles up to 76.9 nm, and also larger angular particles up to 107.7 nm in the slab surface zone. In one sample many larger angular particles were found, more than in the other sample. This was assumed to be the sign of heterogeneity of precipitation in the slab surface zone. Electron diffraction of replicas and EDX analysis confirmed particles TiN and TiC. For steel cast at the high pulling rate 0.8m/min, the particles in the slab surface zone were similar, but finer. Diffraction showed particles of NbC combined with TiN, and TiC.
2. Transmission electron microscopy showed dispersed globular and oval particles 3 mm deep in the slab surface zone, in all 3 cut-outs made from TiNb IF steel cast with high pulling rate 0.8m/min. Fine globular and oval particles from 28 to 85.7 nm in size were evaluated in cut-out 1 and from 14 to 85.7 nm in central cut-out 3, and in the case of

right side cut-out 2, very fine particles ranging from 4.1 to 41.6 nm were found together with larger particles from 57.1 to 100 nm. All of these were identified as nitrides of Al and Ti, or as complex particles based on Al and Ti, in large particles combined sometimes with MnS. Deeper under the surface (20 mm) stick-shape particles were also seen in central side cut-out 3, and precipitates arranged in strings were found in right side cut-out 2. In this side cut-out 2, cementite particles were primarily identified as well. Electron microscopy of the precipitates showed that interstitially solved carbon and nitrogen atoms are bonded to Ti in combination with Al. Unambiguous confirmation of the bonds in all interstitials calls for further analyses, e.g. with chemical phase analysis methods.

3. Comparison of precipitates in the surface zone of slabs cast at the same pulling rate 0.8m/min for both TiNb micro-alloyed steel and TiNb IF steel grades, showed fewer particles in the IF steel. This is assumed to be due to the very low carbon content in the IF steel compared to the microalloyed one. However, this calls for further TEM-assisted particle evaluation with a larger statistically significant numbers of samples.

Acknowledgement

This work was supported by the Joint Scientific Grant Agency (VEGA) of the Slovak Ministry of Education and the Slovak Academy of Sciences, Project No.1/0513/08.

References

[1] V. Ludlow.: Understanding the role of microalloy precipitates in the surface cracking of continuously cast slab, Acta Metallurgica Slovaca, Special Issue 1, Vol. 13, 2007, p. 48-57.
[2] M. Longauerová.: Segregation and precipitation during continuous casting, first ed., TU HF Košice, 2006, ISBN 80-8073-512-3 (in Slovak).
[3] N. A. McPherson, A. McLean: Continuous Casting, Volume 8, Transverse cracking in continuously cast products, The Iron and Steel Society, 1997.
[4] B. Mintz: The influence of composition on the hot ductility of steels and to the problem of transverse cracking, ISIJ International, Vol.39, 1999, No.9, p. 833-855.
[5] M. Longauerová, S. Longauer, R. Mišičko: Precipitation and recrystallization in austenite of Nb-V microalloyed steel, Materials Science Forum, Vols. 113-115, 1993, p. 485-490.
[6] H. L. Andrade, M. G. Akben, J. J. Jonas: Metal. Trans. Vol. 14A, 1983, p. 1967-1977.
[7] J. M. White, W. S. Owen: Metallurg. Trans. Vol. 11A, 4, 1980, p. 597-604.
[8] H. Brunckova, F. Kovac: Thermodynamic conditions and precipitation kinetics of particles in deep-drawn IF steels (in Slovak), Kovové materiály – Metallic Materials, Vol.40, 2002, No.1, p. 53-63.
[9] W. M. Rainforth, C. M. Sellars: Acta Mater., Vol. 50, 2002, p. 735-747.
[10] M. J. Luton, R. Dorvel, R. A. Petkovic: Metallurg. Trans. Vol. 11A, 1980, p. 411-420.
[11] I. C. Jung et al.: ISIJ International, Vol. 35, 1995, No. 8, p. 1001-1005.
[12] S. F. Medina et al.: Influence of Ti and N contents on austenite grain control and precipitate size in structural steel, ISIJ International, vol. 39, 1999, No. 9, p.930-936.
[13] S. Kanazawa et al.: Trans. Iron Steel Inst. Japan, Vol. 16, 1976, p. 486-495.
[14] G. R. Wang et al.: Metall. Trans. Vol. 20A, 1989, p. 2093-2100.
[15] S. J. Rege et al.: ISIJ International, Vol.40, 2000, No.2, p. 191-199.

[16] S. Shanmugam, M. Tanniru, R. D. K. Misra, D. Panda, S. Jansto: Materials Science and Technology, Vol. 21, 2005, No.2, p. 165-177.
[17] Z. Chen, M. H. Loretto, R. C. Cochrane: Materials Science and Technology, Vol. 3, 1987, October, p. 836-844.
[18] H. J. Jun, K. B. Kang, C. G. Park: Scripta Mater., Vol. 49, 2003, p. 1081-1086.
[19] H. R. Wang, W. J. Wang: J. Mater. Sci., Vol. 44, 2009, p. 591-600.